Release Note for `HiggsSignals-1.1`

P. Bechtle, S. Heinemeyer, O.Stål, T. Stefaniak*, G. Weiglein

November 13, 2013

In this note we briefly describe the new features of `HiggsSignals` [1] version 1.1, including information on their implementation and usage. A few examples illustrating some of these features are provided. Furthermore, we give an overview of the default observable set of this version, containing the most up-to-date signal strength measurements as of November 2013.

1 New features in `HiggsSignals-1.1`

1.1 A framework for changed signal efficiencies

The Higgs boson signal rate, $\hat{\mu}_i$, measured in a Higgs analysis i, is typically presented as a quantity, that is normalized to the corresponding predicted signal rate in the Standard Model (SM):

$$\mu_i = \frac{\sum_j \epsilon^j_{\text{model},i} \, [\sigma \times \text{BR}]^j_{\text{model}}}{\sum_j \epsilon^j_{\text{SM},i} \, [\sigma \times \text{BR}]^j_{\text{SM}}} \tag{1}$$

Here, $[\sigma \times \text{BR}]^j$ denote the signal rate (production cross section times branching ratio) of the signal topology j included in the Higgs analysis i. For an inclusive LHC measurement targeting a single Higgs boson decay mode, the signal topologies are typically the five LHC production modes, $j \in \{\text{ggF}, \text{VBF}, WH, ZH, t\bar{t}H\}$. The signal efficiencies/acceptances ϵ^j_i of these signal topologies are defined as the fraction of simulated events, that pass all signal selection criteria. In `HiggsSignals-1.0`, the approximation $\epsilon^j_{\text{model},i} \approx \epsilon^j_{\text{SM},i}$ was employed, restricting the application to models with a SM-like tensor structure of the Higgs boson interactions.

We now introduce *relative efficiency scale factors* $\zeta^j_i \equiv \epsilon^j_{\text{model},i}/\epsilon^j_{\text{SM},i}$, describing the relative change of the signal efficiency in the model with respect to the SM. These factors typically have to be evaluated externally by a Monte-Carlo simulation, where the signal topologies j of both the SM and the model parameter point under investigation need to be confronted with the event selection of the Higgs analysis i. Note again, that ζ^j_i does not contain cross section information. The signal strength, Eq. (1), can now be expressed as

$$\mu_i = \sum_j \zeta^j_i \, \omega^j_{\text{SM},i} \, c^j, \tag{2}$$

*Electronic address: `tim@th.physik.uni-bonn.de`

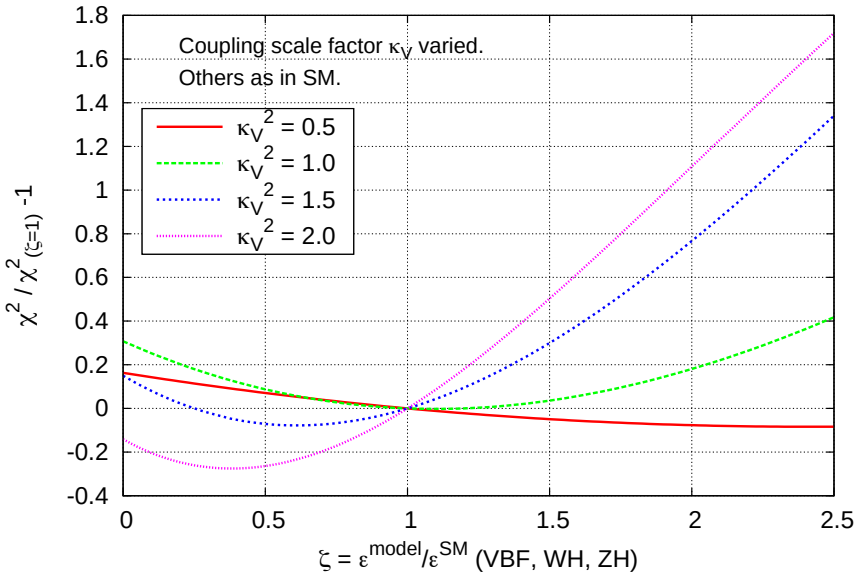

Figure 1: Relative overall χ^2 variation as a function of a common signal efficiency scale factor ζ affecting all channels containing the VBF, WH and ZH production modes. The result is given for four choices of the Higgs-vector boson coupling scale factor, κ_V ($V = W, Z$), whereas the remaining couplings are set to those in the SM. This figure is produced by the example program `HS_efficiencies.f90`.

where we introduced the *SM channel weights* and *individual channel signal strengths*,

$$\omega^j_{\mathrm{SM},i} = \frac{\epsilon^j_{\mathrm{SM},i}\,[\sigma \times \mathrm{BR}]^j_{\mathrm{SM}}}{\sum_{j'} \epsilon^{j'}_{\mathrm{SM},i}\,[\sigma \times \mathrm{BR}]^{j'}_{\mathrm{SM}}}, \qquad c^j = \frac{[\sigma \times \mathrm{BR}]^j_{\mathrm{model}}}{[\sigma \times \mathrm{BR}]^j_{\mathrm{SM}}}, \tag{3}$$

respectively [1].

In `HiggsSignals-1.1` the user can set the relative efficiency scale factors ζ^j_i for each tested parameter point and each signal strength observable i by calling the subroutine:

```
assign_modelefficiencies_to_peak(int obsID, int Nc, double(Nc) zeta)
```

Here, the according observable is specified by the observable ID (`obsID`) and the total number of signal topologies considered in the analysis has to be specified by `Nc`. The efficiency scale factors are then passed as the array `zeta` of the size of `Nc`. The usage is analogous to how toy observables can be set in `HiggsSignals`, cf. Ref. [1].

`HiggsSignals-1.1` contains also a new example program, `HS_efficiencies.f90`, demonstrating this new feature. For four choices of the Higgs boson-vector boson coupling scale factor, κ_V ($V = W, Z$) [2], the total χ^2 is evaluated using the latest experimental data, cf. Section 2, as a function of a common signal efficiency scale factor ζ, affecting all signal topologies containing the VBF, WH or ZH production mode. This χ^2 is normalized to the value obtained for unchanged efficiencies ($\zeta = 1$), and subtracted by 1 for better illustration of the relative change. The fact that the χ^2 minimum for $\kappa_V = 1$ (SM) is located very close

Higgs decay mode	channel code	theo. uncertainty
$H \to \gamma\gamma$	1	5.4 %
$H \to WW$	2	4.8 %
$H \to ZZ$	3	4.8 %
$H \to \tau\tau$	4	6.1 %
$H \to b\bar{b}$	5	2.8 %
$H \to Z\gamma$	6	9.0 %
$H \to c\bar{c}$	7	12.2 %
$H \to \mu\mu$	8	6.0 %
$H \to gg$	9	10.0 %

Table 1: Extended list of Higgs decay modes, including their channel code within `HiggsSignals-1.1` and default maximum theoretical uncertainty in the SM [4].

to $\zeta = 1$ illustrates the remarkably good agreement of present data with the SM hypothesis. Models with reduced signal rates, e.g. for $\kappa_V = 0.5$, favor an increased signal efficiency $\zeta > 1$, and conversely, model with increased signal rates, $\kappa_V = 1.5,\ 2.0$, prefer a reduced signal efficiency $\zeta < 1$. For SM-like signal rates, relative χ^2 changes of the order of 20% are obtained if the signal efficiency is improved by a factor of 2.

1.2 Extension to more Higgs decay channels

We extended the internal `HiggsSignals` structure [1, 3] to accommodate for more than the five most important Higgs decay modes at the LHC. The list of all decay modes, their internal identifiers (or channel codes), and their maximum theoretical uncertainty in the SM as estimated by the LHC Higgs cross section working group (LHC HXSWG) [4] for a Higgs boson mass ~ 125 GeV are given in Tab. 1.

1.3 Treatment of correlated theoretical rate uncertainties

In `HiggsSignals-1.1` the default implementation of the uncertainties of the predicted Higgs boson production cross sections and branching ratios takes into account the correlations induced by common (parametric and theoretical) error sources [4] and, in the latter case, the total decay width. These correlations are evaluated by a Monte Carlo simulation, which can be run by the user via the provided `ROOT` macros:

```
supplements/smearErrorsXS.cpp
supplements/smearErrorsBR.cpp
```

The uncertainties can be treated either as Gaussian or uniform errors. Various parametric and/or theory uncertainty sources can optionally be treated as fully correlated in order to obtain a maximum estimate of the uncertainty. The macros then evaluate the covariance matrix for the cross sections and branching ratios, respectively, given in the basis defined by the `HiggsSignals` channel codes, see Tab. 1 and Ref. [1].

The resulting covariance matrices containing the *relative* uncertainties in the SM and the tested model parameter point are fed into `HiggsSignals-1.1` by including the textfiles

`XScovSM.in`, `XScov.in`,
`BRcovSM.in`, `BRcov.in`,

in the main `HiggsSignals` directory. Per default, the matrices for the SM and the model are identical, however, the user may re-evaluate the model covariance matrix using the provided `ROOT` macros for the tested model parameter point in case of different theoretical uncertainties. In the case that these textfiles are not present in the `HiggsSignals` main directory, the (uncorrelated) maximum uncertainty estimates, cf. Tab. 1 and Ref. [1], are used as in `HiggsSignals-1.0.0`. Furthermore, the user may switch on [off] the usage of these covariance matrices by calling the subroutine

```
setup_correlated_rate_uncertainties(int corr)
```

by setting the argument `corr = 1 [0]`. They are used by default.

If the relative covariance matrices for the production cross sections and branching ratios, denoted in the following by $C^{\text{SM, model}}_{\sigma,ij}$ and $C^{\text{SM, model}}_{\text{BR},ij}$ for the SM and the model, respectively, are provided, the contribution to the overall covariance matrix from the theoretical uncertainties of the predicted signal strength, Eq. (10) in Ref. [1] (see also for notation), changes to

$$\left(\sum_{a=1}^{k_\alpha}\sum_{b=1}^{k_\beta}\left[C^{\text{model}}_{\sigma,p(a)p(b)} + C^{\text{model}}_{\text{BR},d(a)d(b)}\right]\cdot\omega^{\text{model}}_{a,\alpha}\omega^{\text{model}}_{b,\beta}\right)\mu_\alpha\mu_\beta, \tag{4}$$

where now, $\delta_{p(a)p(b)}\Delta\sigma^{\text{model}}_{p(a)}\Delta\sigma^{\text{model}}_{p(b)}$ and $\delta_{d(a)d(b)}\Delta\text{BR}^{\text{model}}_{d(a)}\Delta\text{BR}^{\text{model}}_{d(b)}$ have been replaced by $C^{\text{model}}_{\sigma,ij}$ and $C^{\text{model}}_{\text{BR},ij}$, respectively. The theoretical rate uncertainty of the SM, which is typically already included in the measurement and therefore needs to be subtracted from the $\hat{\mu}$ uncertainty beforehand, is now evaluated in a similar way using $C^{\text{SM}}_{\sigma,ij}$ and $C^{\text{SM}}_{\text{BR},ij}$.

For reference, we give here the correlation matrices for the production cross sections (ggH, VBF, WH, ZH, $t\bar{t}H$) and branching ratios in the SM:

$$(\rho^{\text{SM}}_{\sigma,ij}) = \begin{pmatrix} 1 & -2.0\cdot10^{-3} & 3.7\cdot10^{-3} & 9.0\cdot10^{-3} & 0.524 \\ -2.0\cdot10^{-3} & 1 & 0.658 & 0.439 & 2.5\cdot10^{-3} \\ 3.7\cdot10^{-3} & 0.658 & 1 & 0.866 & -9.8\cdot10^{-5} \\ 9.0\cdot10^{-3} & 0.439 & 0.866 & 1 & 2.8\cdot10^{-3} \\ 0.524 & 2.5\cdot10^{-3} & -9.8\cdot10^{-5} & 2.8\cdot10^{-3} & 1 \end{pmatrix}, \tag{5}$$

$$(\rho^{\text{SM}}_{\text{BR},ij}) = \begin{pmatrix} 1 & 0.96 & 0.96 & 0.86 & -0.94 & 0.60 & -0.19 & 0.86 & 0.71 \\ 0.96 & 1 & 0.98 & 0.88 & -0.96 & 0.61 & -0.19 & 0.88 & 0.73 \\ 0.96 & 0.98 & 1 & 0.88 & -0.96 & 0.61 & -0.19 & 0.88 & 0.73 \\ 0.86 & 0.88 & 0.88 & 1 & -0.89 & 0.55 & -0.18 & 0.79 & 0.65 \\ -0.94 & -0.96 & -0.96 & -0.89 & 1 & -0.60 & 0.16 & -0.85 & -0.83 \\ 0.60 & 0.61 & 0.61 & 0.55 & -0.60 & 1 & -0.10 & 0.55 & 0.45 \\ -0.19 & -0.19 & -0.19 & -0.18 & 0.16 & -0.10 & 1 & -0.20 & -0.55 \\ 0.86 & 0.88 & 0.88 & 0.79 & -0.85 & 0.55 & -0.20 & 1 & 0.65 \\ 0.71 & 0.73 & 0.73 & 0.65 & -0.83 & 0.45 & -0.55 & 0.65 & 1 \end{pmatrix}. \tag{6}$$

1.4 Other developments

There are a few more new subroutines that give the user more control over the details of the model test. Here, we only give an overview of the new subroutines and functionalities, and refer to Ref. [1] for the meaning and definition of the parameters.

The assignment range Λ, which is an important tuning parameter for the automatic assignment procedure of Higgs bosons to the peak observables, can now be specified separately for mass-sensitive and mass-insensitive observables, i.e. peak observables, which either contain or do not contain a mass measurement. While the old routine `setup_assignmentrange` affects all observables, the new subroutine

```
setup_assignmentrange_massobservables(double Lambda)
```

sets the assignment range (`Lambda`) for only the mass sensitive observables.

More control over the way experimental uncertainties of the signal strength measurements, $\Delta\hat{\mu}$, are interpreted within `HiggsSignals` is provided by the subroutines

```
setup_absolute_errors(int absol)
```

and

```
setup_symmetric_errors(int symm)
```

where the quoted uncertainties can be interpreted as relative or absolute errors (`absol = 0,1`) and treated as either asymmetric or symmetric (i.e. an average of the upper and lower band uncertainty) uncertainties (`symm = 0,1`). By default, `HiggsSignals` treats the uncertainties as relative, asymmetric Gaussian errors.

2 New experimental analyses

We list the full set of peak observables included in the `latestresults` observable set of `HiggsSignals-1.1` in Tabs. 2 and 3.

Analysis	energy $\sqrt{s}$	$\hat{\mu} \pm \Delta\hat{\mu}$	SM signal composition [in %]				
			ggH	VBF	WH	ZH	$t\bar{t}H$
ATL $(pp) \to h \to WW \to \ell\nu\ell\nu$ (0/1jet) [5, 6]	7/8 TeV	$0.82^{+0.33}_{-0.32}$	97.2	1.6	0.7	0.4	0.1
ATL $(pp) \to h \to WW \to \ell\nu\ell\nu$ (VBF) [5, 6]	7/8 TeV	$1.42^{+0.70}_{-0.56}$	19.8	80.2	0.0	0.0	0.0
ATL $(pp) \to h \to ZZ \to 4\ell$ (VBF/VH-like) [7, 6]	7/8 TeV	$1.18^{+1.64}_{-0.90}$	36.8	43.1	12.8	7.3	0.0
ATL $(pp) \to h \to ZZ \to 4\ell$ (ggH-like) [7, 6]	7/8 TeV	$1.45^{+0.43}_{-0.37}$	92.5	4.5	1.9	1.1	0.0
ATL $(pp) \to h \to \gamma\gamma$ (unconv.-central-low p_{Tt}) [8]	7 TeV	$0.53^{+1.41}_{-1.48}$	92.9	3.8	2.0	1.1	0.2
ATL $(pp) \to h \to \gamma\gamma$ (unconv.-central-high p_{Tt}) [8]	7 TeV	$0.22^{+1.94}_{-1.95}$	65.5	14.8	10.8	6.2	2.7
ATL $(pp) \to h \to \gamma\gamma$ (unconv.-rest-low p_{Tt}) [8]	7 TeV	$2.52^{+1.68}_{-1.68}$	92.6	3.7	2.2	1.2	0.2
ATL $(pp) \to h \to \gamma\gamma$ (unconv.-rest-high p_{Tt}) [8]	7 TeV	$10.44^{+3.67}_{-3.70}$	64.4	15.2	11.8	6.6	2.0
ATL $(pp) \to h \to \gamma\gamma$ (conv.-central-low p_{Tt}) [8]	7 TeV	$6.10^{+2.63}_{-2.62}$	92.7	3.8	2.1	1.1	0.2
ATL $(pp) \to h \to \gamma\gamma$ (conv.-central-high p_{Tt}) [8]	7 TeV	$-4.36^{+1.80}_{-1.81}$	65.7	14.4	11.0	6.2	2.8
ATL $(pp) \to h \to \gamma\gamma$ (conv.-rest-low p_{Tt}) [8]	7 TeV	$2.74^{+1.98}_{-2.01}$	92.7	3.6	2.2	1.2	0.2
ATL $(pp) \to h \to \gamma\gamma$ (conv.-rest-high p_{Tt}) [8]	7 TeV	$-1.59^{+2.89}_{-2.90}$	64.4	15.1	12.1	6.4	2.0
ATL $(pp) \to h \to \gamma\gamma$ (conv.-trans.) [8]	7 TeV	$0.37^{+3.58}_{-3.79}$	89.2	5.0	3.7	1.9	0.3
ATL $(pp) \to h \to \gamma\gamma$ (2 jet) [8]	7 TeV	$2.72^{+1.87}_{-1.85}$	23.3	75.9	0.5	0.2	0.1
ATL $(pp) \to h \to \gamma\gamma$ (unconv.-central-low p_{Tt}) [9]	8 TeV	$0.87^{+0.73}_{-0.70}$	92.0	5.0	1.7	0.8	0.5
ATL $(pp) \to h \to \gamma\gamma$ (unconv.-central-high p_{Tt}) [9]	8 TeV	$0.96^{+1.07}_{-0.95}$	78.6	12.6	4.7	2.6	1.4
ATL $(pp) \to h \to \gamma\gamma$ (unconv.-rest-low p_{Tt}) [9]	8 TeV	$2.50^{+0.92}_{-0.77}$	92.0	5.0	1.7	0.8	0.5
ATL $(pp) \to h \to \gamma\gamma$ (unconv.-rest-high p_{Tt}) [9]	8 TeV	$2.69^{+1.35}_{-1.17}$	78.6	12.6	4.7	2.6	1.4
ATL $(pp) \to h \to \gamma\gamma$ (conv.-central-low p_{Tt}) [9]	8 TeV	$1.39^{+1.01}_{-0.95}$	92.0	5.0	1.7	0.8	0.5
ATL $(pp) \to h \to \gamma\gamma$ (conv.-central-high p_{Tt}) [9]	8 TeV	$1.98^{+1.54}_{-1.26}$	78.6	12.6	4.7	2.6	1.4
ATL $(pp) \to h \to \gamma\gamma$ (conv.-rest-low p_{Tt}) [9]	8 TeV	$2.23^{+1.14}_{-1.01}$	92.0	5.0	1.7	0.8	0.5
ATL $(pp) \to h \to \gamma\gamma$ (conv.-rest-high p_{Tt}) [9]	8 TeV	$1.27^{+1.32}_{-1.23}$	78.6	12.6	4.7	2.6	1.4
ATL $(pp) \to h \to \gamma\gamma$ (conv.-trans.) [9]	8 TeV	$2.78^{+1.72}_{-1.57}$	92.0	5.0	1.7	0.8	0.5
ATL $(pp) \to h \to \gamma\gamma$ (high mass, 2 jet, loose) [9]	8 TeV	$2.75^{+1.78}_{-1.38}$	45.3	53.7	0.5	0.3	0.2
ATL $(pp) \to h \to \gamma\gamma$ (high mass, 2 jet, tight) [9]	8 TeV	$1.61^{+0.83}_{-0.67}$	27.1	72.5	0.3	0.1	0.0
ATL $(pp) \to h \to \gamma\gamma$ (low mass, 2 jet) [9]	8 TeV	$0.32^{+1.72}_{-1.44}$	38.0	2.9	40.1	16.9	2.1
ATL $(pp) \to h \to \gamma\gamma$ (E_T^{miss} sign.) [9]	8 TeV	$2.97^{+2.71}_{-2.15}$	4.4	0.3	35.8	47.4	12.2
ATL $(pp) \to h \to \gamma\gamma$ (1ℓ) [9]	8 TeV	$2.69^{+1.97}_{-1.66}$	2.5	0.4	63.3	15.2	18.7
ATL $(pp) \to h \to \tau\tau$ [10, 11]	7/8 TeV	$0.77^{+0.70}_{-0.65}$	88.1	7.1	3.1	1.7	0.0
ATL $(pp) \to Vh \to V(bb)$ (0ℓ) [12]	7/8 TeV	$0.46^{+0.88}_{-0.86}$	0.0	0.0	21.2	78.8	0.0
ATL $(pp) \to Vh \to V(bb)$ (1ℓ) [12]	7/8 TeV	$0.09^{+1.01}_{-1.00}$	0.0	0.0	96.7	3.3	0.0
ATL $(pp) \to Vh \to V(bb)$ (2ℓ) [12]	7/8 TeV	$-0.36^{+1.48}_{-1.38}$	0.0	0.0	0.0	100.0	0.0
ATL $(pp) \to Vh \to V(WW)$ [13]	7/8 TeV	$3.70^{+1.90}_{-2.00}$	0.0	0.0	63.8	36.2	0.0
CDF $(p\bar{p}) \to h \to WW$ [14]	1.96 TeV	$0.00^{+1.78}_{-1.78}$	77.5	5.4	10.6	6.5	0.0
CDF $(p\bar{p}) \to h \to \gamma\gamma$ [14]	1.96 TeV	$7.81^{+4.61}_{-4.42}$	77.5	5.4	10.6	6.5	0.0
CDF $(p\bar{p}) \to h \to \tau\tau$ [14]	1.96 TeV	$0.00^{+8.44}_{-8.44}$	77.5	5.4	10.6	6.5	0.0
CDF $(p\bar{p}) \to Vh \to Vbb$ [14]	1.96 TeV	$1.72^{+0.92}_{-0.87}$	0.0	0.0	61.9	38.1	0.0
CDF $(p\bar{p}) \to tth \to ttbb$ [14]	1.96 TeV	$9.49^{+6.60}_{-6.28}$	0.0	0.0	0.0	0.0	100.0

Table 2: Peak observables from ATLAS and CDF included in the default observable set `latestresults` in `HiggsSignals-1.1`.

Analysis	energy $\sqrt{s}$	$\hat{\mu} \pm \Delta\hat{\mu}$	SM signal composition [in %]				
			ggH	VBF	WH	ZH	$t\bar{t}H$
CMS $(pp) \to h \to WW$ (0/1 jet) [15]	7/8 TeV	$0.77^{+0.17}_{-0.24}$	95.0	5.0	0.0	0.0	0.0
CMS $(pp) \to h \to WW$ (VBF) [16]	7/8 TeV	$0.62^{+0.58}_{-0.47}$	19.8	80.2	0.0	0.0	0.0
CMS $(pp) \to Vh \to V(WW)$ (hadronic V) [17]	7/8 TeV	$1.00^{+2.00}_{-2.00}$	59.8	4.0	24.2	12.0	0.0
CMS $(pp) \to Wh \to W(WW) \to 3\ell 3\nu$ [18]	7/8 TeV	$0.51^{+1.26}_{-0.94}$	0.0	0.0	100[1]	0.0	0.0
CMS $(pp) \to h \to ZZ \to 4\ell$ (0/1 jet) [19]	7/8 TeV	$0.86^{+0.32}_{-0.26}$	89.8	10.2	0.0	0.0	0.0
CMS $(pp) \to h \to ZZ \to 4\ell$ (2 jet) [19]	7/8 TeV	$1.24^{+0.85}_{-0.58}$	71.2	28.8	0.0	0.0	0.0
CMS $(pp) \to h \to \gamma\gamma$ (untagged 0) [20, 21]	7 TeV	$3.88^{+2.00}_{-1.68}$	61.4	16.9	12.0	6.6	3.1
CMS $(pp) \to h \to \gamma\gamma$ (untagged 1) [20, 21]	7 TeV	$0.20^{+1.01}_{-0.93}$	87.7	6.2	3.6	2.0	0.5
CMS $(pp) \to h \to \gamma\gamma$ (untagged 2) [20, 21]	7 TeV	$0.04^{+1.25}_{-1.24}$	91.4	4.4	2.5	1.4	0.3
CMS $(pp) \to h \to \gamma\gamma$ (untagged 3) [20, 21]	7 TeV	$1.47^{+1.68}_{-2.47}$	91.3	4.4	2.6	1.5	0.2
CMS $(pp) \to h \to \gamma\gamma$ (2 jet) [20, 21]	7 TeV	$4.18^{+2.31}_{-1.78}$	26.7	72.6	0.4	0.2	0.0
CMS $(pp) \to h \to \gamma\gamma$ (untagged 0) [21]	8 TeV	$2.20^{+0.95}_{-0.78}$	72.9	11.7	8.2	4.6	2.6
CMS $(pp) \to h \to \gamma\gamma$ (untagged 1) [21]	8 TeV	$0.06^{+0.69}_{-0.67}$	83.5	8.5	4.5	2.6	1.0
CMS $(pp) \to h \to \gamma\gamma$ (untagged 2) [21]	8 TeV	$0.31^{+0.50}_{-0.47}$	91.5	4.5	2.3	1.3	0.4
CMS $(pp) \to h \to \gamma\gamma$ (untagged 3) [21]	8 TeV	$-0.36^{+0.88}_{-0.81}$	92.5	3.9	2.1	1.2	0.3
CMS $(pp) \to h \to \gamma\gamma$ (2 jet, tight) [21]	8 TeV	$0.27^{+0.69}_{-0.58}$	20.6	79.0	0.2	0.1	0.1
CMS $(pp) \to h \to \gamma\gamma$ (2 jet, loose) [21]	8 TeV	$0.78^{+1.10}_{-0.98}$	46.8	51.1	1.1	0.6	0.5
CMS $(pp) \to h \to \gamma\gamma$ (μ) [21]	8 TeV	$0.38^{+1.84}_{-1.36}$	0.0	0.2	50.4	28.6	20.8
CMS $(pp) \to h \to \gamma\gamma$ (e) [21]	8 TeV	$-0.67^{+2.78}_{-1.95}$	1.1	0.4	50.2	28.5	19.8
CMS $(pp) \to h \to \gamma\gamma$ ($E_T^{\rm miss}$) [21]	8 TeV	$1.89^{+2.62}_{-2.28}$	22.1	2.6	40.6	23.0	11.7
CMS $(pp) \to h \to \mu\mu$ [22]	7/8 TeV	$2.90^{+2.80}_{-2.70}$	92.5	7.5	0.0	0.0	0.0
CMS $(pp) \to h \to \tau\tau(0/1jet)$ [23]	7/8 TeV	$0.77^{+0.58}_{-0.55}$	95.0	5.0	0.0	0.0	0.0
CMS $(pp) \to h \to \tau\tau$ (VBF) [23]	7/8 TeV	$1.42^{+0.70}_{-0.64}$	19.8	80.2	0.0	0.0	0.0
CMS $(pp) \to Vh \to V(bb)$ [24]	7/8 TeV	$1.00^{+0.51}_{-0.49}$	0.0	0.0	63.8	36.2	0.0
CMS $(pp) \to Vh \to V(\tau\tau)$ [23]	7/8 TeV	$0.98^{+1.68}_{-1.50}$	0.0	0.0	17.2	9.8	0.0
CMS $(pp) \to tth \to 2\ell$ (same-sign) [25]	8 TeV	$5.30^{+2.20}_{-1.80}$	0.0	0.0	0.0	0.0	100.0[2]
CMS $(pp) \to tth \to 3\ell$ [25]	8 TeV	$2.70^{+2.20}_{-1.80}$	0.0	0.0	0.0	0.0	100.0[3]
CMS $(pp) \to tth \to 4\ell$ [25]	8 TeV	$-4.80^{+5.00}_{-1.20}$	0.0	0.0	0.0	0.0	100.0[4]
CMS $(pp) \to tth \to tt(bb)$ [26]	7/8 TeV	$1.00^{+1.90}_{-2.00}$	0.0	0.0	0.0	0.0	100.0
CMS $(pp) \to tth \to tt(\tau\tau)$ [26]	8 TeV	$-1.40^{+6.30}_{-5.50}$	0.0	0.0	0.0	0.0	100.0
CMS $(pp) \to tth \to tt(\gamma\gamma)$ [27]	8 TeV	$-0.20^{+2.40}_{-1.90}$	0.0	0.0	0.0	0.0	100.0
D0 $(p\bar{p}) \to h \to WW$ [28]	1.96 TeV	$1.90^{+1.63}_{-1.52}$	77.5	5.4	10.6	6.5	0.0
D0 $(p\bar{p}) \to h \to bb$ [28]	1.96 TeV	$1.23^{+1.24}_{-1.17}$	0.0	0.0	61.9	38.1	0.0
D0 $(p\bar{p}) \to h \to \gamma\gamma$ [28]	1.96 TeV	$4.20^{+4.60}_{-4.20}$	77.5	5.4	10.6	6.5	0.0
D0 $(p\bar{p}) \to h \to \tau\tau$ [28]	1.96 TeV	$3.96^{+4.11}_{-3.38}$	77.5	5.4	10.6	6.5	0.0

[1] The signal is contaminated to 12.0% by $WH \to W(\tau\tau)$ in the SM.
[2] The $t\bar{t}h \to \ell^\pm\ell^\pm$ signal is comprised of the final states WW (74.5%), ZZ (3.7%) and $\tau\tau$ (21.7%) in the SM.
[3] The $t\bar{t}h \to 3\ell$ signal is comprised of the final states WW (73.0%), ZZ (4.6%) and $\tau\tau$ (22.5%) in the SM.
[4] The $t\bar{t}h \to 4\ell$ signal is comprised of the final states WW (54.1%), ZZ (17.4%) and $\tau\tau$ (28.5%) in the SM.

Table 3: Peak observables from CMS and DØ included in the default observable set `latestresults` in `HiggsSignals-1.1`.

References

[1] P. Bechtle, S. Heinemeyer, O. Stål, T. Stefaniak, and G. Weiglein arXiv:1305.1933.

[2] LHC Higgs Cross Section Working Group, A. David *et. al.* arXiv:1209.0040.

[3] P. Bechtle, O. Brein, S. Heinemeyer, G. Weiglein, and K. E. Williams *Comput. Phys. Commun.* **181** (2010) 138–167, [arXiv:0811.4169]; P. Bechtle, O. Brein, S. Heinemeyer, G. Weiglein, and K. E. Williams *Comput. Phys. Commun.* **182** (2011) 2605–2631, [arXiv:1102.1898]; P. Bechtle, O. Brein, S. Heinemeyer, O. Stål, T. Stefaniak, G. Weiglein, and K. E. Williams arXiv:1301.2345; P. Bechtle, O. Brein, S. Heinemeyer, O. Stål, T. Stefaniak, *et. al.* arXiv:1311.0055.

[4] LHC Higgs Cross Section Working Group, S. Heinemeyer *et. al.* arXiv:1307.1347.

[5] ATLAS Collaboration. ATLAS-CONF-2013-030.

[6] ATLAS Collaboration, G. Aad *et. al. Phys.Lett.* **B726** (2013) 88–119, [arXiv:1307.1427].

[7] ATLAS Collaboration. ATLAS-CONF-2013-013.

[8] ATLAS Collaboration. ATLAS-CONF-2012-091.

[9] ATLAS Collaboration. ATLAS-CONF-2013-012.

[10] ATLAS Collaboration. ATLAS-CONF-2013-034.

[11] ATLAS Collaboration. ATLAS-CONF-2012-160.

[12] ATLAS collaboration. ATLAS-CONF-2013-079, ATLAS-COM-CONF-2013-080.

[13] ATLAS collaboration. ATLAS-CONF-2013-075, ATLAS-COM-CONF-2013-069.

[14] CDF Collaboration, T. Aaltonen *et. al.* arXiv:1301.6668.

[15] CMS Collaboration. CMS-PAS-HIG-13-003.

[16] CMS Collaboration. CMS-PAS-HIG-13-022.

[17] CMS Collaboration. CMS-PAS-HIG-13-017.

[18] CMS Collaboration. CMS-PAS-HIG-13-009.

[19] CMS Collaboration. CMS-PAS-HIG-13-002.

[20] CMS Collaboration. CMS-PAS-HIG-12-015.

[21] CMS Collaboration. CMS-PAS-HIG-13-001.

[22] CMS Collaboration. CMS-PAS-HIG-13-007.

[23] CMS Collaboration. CMS-PAS-HIG-13-004.

[24] CMS Collaboration. CMS-PAS-HIG-13-012.

[25] CMS Collaboration. CMS-PAS-HIG-13-020.

[26] CMS Collaboration. CMS-PAS-HIG-13-019.

[27] CMS Collaboration. CMS-PAS-HIG-13-015.

[28] DØ Collaboration, V. M. Abazov *et. al.* arXiv:1303.0823.